JOURNAL OF THERMOPHYSICS AND HEAT TRANSFER
Vol. 20, No. 4, October–December 2006

Development and Test Results of a Dual Compensation Chamber Loop Heat Pipe

Lin Guiping* and Zhang Hongxing†
Beihang University, 100083 Beijing, People's Republic of China
and
Shao Xingguo,‡ Cao Jianfeng,§ Ding Ting,‖ and Miao Jianyin¶
China Academy of Space Technology, 100086 Beijing, People's Republic of China

DOI: 10.2514/1.21858

A dual compensation chamber loop heat pipe is developed to solve the problem of the relative orientation limit between the evaporator and the compensation chambers. The construction of the evaporator and the compensation chambers is presented. The concurrent design method of the working fluid charge mass and the compensation chamber volumes, that can realize the objectives where, within a certain temperature range, the dual compensation chamber loop heat pipe cannot only start up and operate normally at any orientation, but can also avoid the most difficult startup situation, is introduced. The operation and the thermal control characteristics of the dual compensation chamber loop heat pipe are investigated. Test results indicate that in some heat load regions, the operating temperatures vary with the relative orientation between the evaporator and the compensation chambers. This is explained by the thermal equilibrium of the compensation chamber and the usage efficiency of the return liquid subcooling. The test results and discussion of the dual compensation chamber loop heat pipe suggest that part of the return liquid subcooling that cools the liquid to be locally subcooled must be considered in the mathematical modeling of the loop heat pipe.

Nomenclature

A	=	area, m^2
$c_{p,l}$	=	specific heat at constant pressure, $J/kg \cdot K$
E	=	thermodynamic energy, J
h	=	specific enthalpy, J/kg
m	=	charge mass of the working fluid, kg
p	=	pressure, Pa
Q	=	heat load, W
R	=	radius, m
T	=	temperature, K
V	=	volume, m^3
v	=	specific volume, m^3/kg
α	=	fraction of compensation chamber volume occupied by the liquid under the hot case
β	=	fraction of compensation chamber volume occupied by the liquid under the cold case
Δ	=	difference
η	=	effective usage efficiency of the subcooling of the returning liquid
ρ	=	density, kg/m^3
χ	=	coefficient to measure the effect of liquid subcooling on the thermal equilibrium in the saturated compensation chamber

Subscripts

amb	=	ambience
bay	=	bayonet
CC 1	=	compensation chamber without the bayonet inside
CC 2	=	compensation chamber with the bayonet inside
cond	=	condenser
eff	=	effective
evap	=	evaporator
fg	=	difference of thermal properties between saturated fluid and gas
HL	=	heat leak
LC	=	liquid core
LL	=	liquid line
sat	=	saturation or saturated
sink	=	heat sink
sub	=	liquid subcooling
VG	=	vapor groove
VL	=	vapor line
wick	=	primary wick

Received 17 December 2005; revision received 10 April 2006; accepted for publication 11 April 2006.

*Professor, School of Aeronautic Science & Technology, 100083 Beijing, People's Republic of China.
†Doctor, School of Aeronautic Science & Technology, 100083 Beijing, People's Republic of China; redlincoco@hotmail.com.
‡Professor, Heat Pipe Laboratory, P.O. Box 5142, exit 86, 100094 Beijing, People's Republic of China.
§Doctor, Heat Pipe Laboratory, P.O. Box 5142, exit 86, 100094 Beijing, People's Republic of China.
‖Doctor, Heat Pipe Laboratory, P.O. Box 5142, exit 86, 100094 Beijing, People's Republic of China.
¶Professor, Heat Pipe Laboratory, P.O. Box 5142, exit 86, 100094 Beijing, People's Republic of China.

I. Introduction

LOOP heat pipes (LHPs) are promising and valuable two-phase heat transfer devices, which use the evaporation and condensation of the working fluid to transfer heat. Many flight tests have verified the heat transfer ability of LHPs for space application. In microgravity environment, as the secondary wick inside the primary wick, which is usually a set of wire screens, links the liquid core and the compensation chamber (CC), the capillary force provided by the secondary wick can always supply the liquid in the CC to the primary wick in all orientations. However, in the thermal vacuum tests of spacecrafts and other applications in gravity, such as the thermal management system of aircrafts and submarines, the relative orientation of the evaporator and the CC will be limited. Because the liquid will prefer to stay in the CC in gravity when the evaporator is above the CC, as shown in Fig. 1, the limited capillary

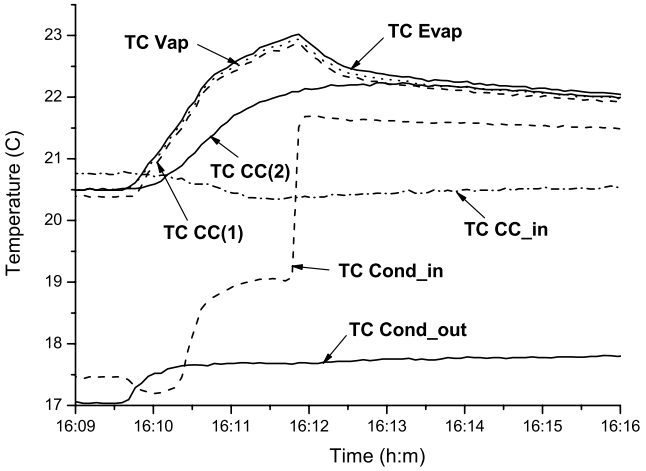

Fig. 2 Startup with the liquid core flooded by liquid [3].

force provided by the secondary wick is not large enough to overcome the gravity and cannot supply the liquid in the CC to the primary wick in gravity. Then, the LHP will fail to start up and operate.

Besides the orientation limit of the evaporator and the CC, the startup is another problem hindering the application of the LHPs. There are four startup situations [1–3], which depend on the liquid-vapor composition in the liquid core and vapor grooves. When the vapor grooves are flooded with liquid, a liquid superheat is required to initiate the nucleate boiling. Then, if the liquid core is flooded with the liquid, the heat leak from the evaporator to the CC by the heat transfer mode of conduction is small. As shown in Fig. 2 [1], the startup is easy. If vapor exists in the liquid core, the link of the liquid core and the CC is like a traditional heat pipe, which will lead to a very high heat leak from the evaporator to the CC. As shown in Fig. 3 [1], the temperature difference between the evaporator and the CC, namely, the liquid superheat, is difficult to attain. In this situation, the startup will last a long time, and the evaporator temperature will rise and maybe exceed the allowable temperature.

However, the dual compensation chamber loop heat pipe (DCCLHP), which has two compensation chambers on the two ends of the evaporator, successfully solves the problem of the liquid supply difficulty for the primary wick in gravity. The Institute of Thermal Physics Ural Branch of the Russian Academy of Sciences has designed a DCCLHP and verified its ability to operate in different orientations [4]. Gluck et al. [5] present the test results in the U.S. Air Force Research Laboratory and analyze the operating temperature differences from the test results in Russia. However, compared with the conventional LHP with a single CC, both the theoretical research and the experimental results of the DCCLHP are inadequate. More detailed investigations are required to characterize the startup and operation of the DCCLHP and optimize the configuration.

In this paper, a DCCLHP is developed to solve the problem of the relative orientation limit and the startup problem. The construction of the evaporator and the CCs is presented. The concurrent design method of the working fluid charge mass and the CC volumes for the DCCLHP is introduced that can realize the objectives where, within a certain temperature range, the DCCLHP cannot only start up and operate normally at any orientation, but also avoid the most difficult startup situation. The operation and the thermal control characteristics of the DCCLHP are investigated. It is found that the operating temperatures in different orientations are close to each other in both the lower heat load region under the variable conductance mode and the heat load region under the constant conductance mode, whereas they are different in the higher heat load region under the variable conductance mode. This is explained by the thermal equilibrium of the CC and the usage efficiency of the return liquid subcooling. The test results and discussion of the DCCLHP also suggest that part of the return liquid subcooling, which has cooled the liquid to be locally subcooled, must be considered in the mathematical modeling of the LHP. Another suggestion is that an effective method to decrease the

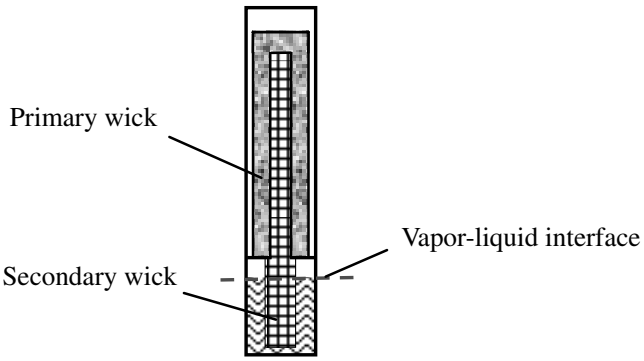

Fig. 1 The unfavorable orientation of LHPs.

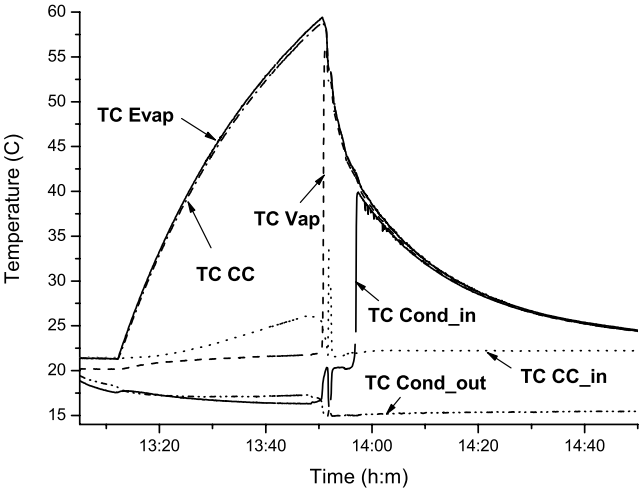

Fig. 3 Startup with vapor in the liquid core [3].

operating temperature or thermal resistance of the DCCLHP is to enhance the heat transfer between the return liquid and the fluid in the saturated CC to increase the usage efficiency of the return liquid subcooling.

II. DCCLHP Design and Test Setup

A. DCCLHP Configuration and Dimensions

The test device was an ammonia-stainless steel DCCLHP with a nickel wick, which was manufactured in the China Academy of Space Technology. The construction of the evaporator and the two CCs is shown in Fig. 4. The bayonet extends to the middle point of the liquid core so that it can push the gas and bubbles out of the liquid core at any orientation. No secondary wick is fixed in the liquid core and the CCs for the ground test. The vapor, liquid, and condenser lines are stainless steel tubes. The condenser line is mounted on an aluminum cold plate with imbedded coolant channels. Table 1 shows the geometric parameters of the components, where o.d. and i.d. represent the outside and inside diameters.

B. Design of the Working Fluid Charge Mass and the CC Volume

The charge mass of the working fluid and the CC volume must be carefully designed, because they affect the maximum conductance, the startup characteristics, and other performances of the LHP. In this paper, the objectives of the working fluid charge mass and the CC volumes design are that, within a certain temperature range, the DCCLHP cannot only start up and operate at any orientation, but also avoid the most difficult startup situation.

Ku [1] introduced the concurrent design method of the working fluid charge mass and the CC volume of the conventional LHP, which can only realize that, within a certain temperature range, the LHP can start up and operate normally at some certain orientations. The two parameters are functions of the operating temperature range

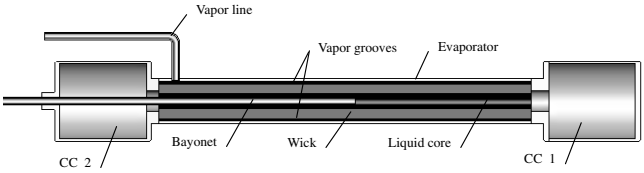

Fig. 4 Construction of the evaporator and the CCs.

and the component dimensions. The design result must meet both the hot condition and the cold condition within a certain temperature range at some certain orientations. In the cold case, namely, at the minimum operating temperature, the working fluid will experience the most contraction and occupy the smallest volume for its increased density. The cold condition demands that, at the minimum temperature, the primary wick in the evaporator be soaked to assure the LHP of the ability to start up and operate even when the external loop is flooded with liquid. In the hot case, namely, at the maximum operating temperature, the working fluid will undergo the most expansion and occupy the greatest volume. The hot condition demands that, at the maximum temperature, the CC can contain the working fluid even when the condenser is fully used at the highest heat load.

However, normal startup does not always satisfy the thermal control requirement in applications. To realize the absolutely passive operation with no auxiliary startup measure, the cold condition must be modified to avoid the most difficult startup situation in the concurrent design of the charge mass and the CC volume. The modified cold condition should demand that, at the minimum temperature, the liquid core be flooded with liquid to assure the LHP of the ability to start up and operate normally and avoid the most difficult startup even when the external loop is flooded with liquid. The modified cold condition and the hot condition can be expressed as Eqs. (1) and (2), respectively,

$$m = \rho_{1,\text{cold}}(\beta V_{\text{CC}} + V_{\text{LL}} + V_{\text{cond}} + \varepsilon V_{\text{wick}} + V_{\text{VL}} + V_{\text{VG}} + V_{\text{LC}}) + \rho_{v,\text{cold}}[(1-\beta)V_{\text{CC}}] \quad (1)$$

$$m = \rho_{1,\text{hot}}(\alpha V_{\text{CC}} + \varepsilon V_{\text{wick}} + V_{\text{LL}} + V_{\text{LC}}) + \rho_{v,\text{hot}}[V_{\text{cond}} + V_{\text{VL}} + V_{\text{VG}} + (1-\alpha)V_{\text{CC}}] \quad (2)$$

In Eqs. (1) and (2), α and β are two fill factors for users to define. α is the percentage of the CC that is liquid filled in the hot case, and $1-\alpha$ is the volume percentage of the CC allowed for noncondensable gas storage at the end of life. β is the percentage of the CC that is liquid filled in the cold case. In the space application of the conventional LHP with a singe CC in microgravity, if the value of β is defined to be 0.5 or even less, the liquid in the CC can be provided to the primary wick at any orientation by the secondary wick, which links the CC and the liquid core. However, in gravity, the liquid will prefer to stay in the CC due to the gravity when the CC is below the evaporator. The conventional LHP cannot meet the cold condition through a suitable β definition. Namely, the LHP with a single CC cannot realize the normal startup and operation without orientation limit through the concurrent design of the working fluid

Table 1 Geometric parameters of the test DCCLHP

Components	Dimensions
o.d./i.d. × length of evaporator/mm	$\Phi 18/16 \times 190$
o.d./i.d. × length of vapor line/mm	$\Phi 3/2 \times 2200$
o.d./i.d. × length of liquid line/mm	$\Phi 3/2 \times 2600$
o.d./i.d. × length of condenser line/mm	$\Phi 3/2.6 \times 2000$
Volume of CC/ml	24.7×2
Charge of working fluid/g	49.1
Maximum radius of wick/μm	1.1
Porosity of wick	55%
Permeability of wick/m^2	$>5 \times 10^{-14}$
o.d./i.d. × length of wick/mm	$16/6 \times 180$
number × height × width of grooves/mm	$6 \times 1 \times 1$

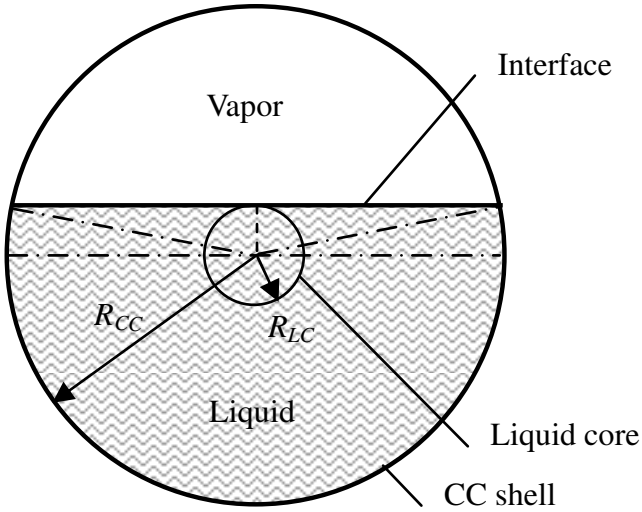

Fig. 5 Section of the liquid core and CC.

charge mass and the CC volume. However, the DCCLHP solves the problem of the liquid gathering in the bottom CC. A suitable β value can even make it possible for the DCCLHP liquid core to be always flooded by liquid at any orientation even in the cold case. Then, DCCLHP would be able to not only start up and operate at any orientation within a certain temperature range, but also avoid the most difficult startup situation.

In the DCCLHP design, β can be defined as the total volume percentage of the two CCs that are liquid filled in the cold case. To satisfy the cold condition and avoid the most difficult startup situation at any orientation, the liquid core must at least be flooded by liquid in two typical orientations, namely, the vertical and the horizontal orientations. Then, two β values for the two typical orientations can be obtained. The larger β value can satisfy the modified cold situation at any orientation.

In the vertical orientation, the liquid must flood the liquid core and the bottom CC. As one of the CCs will be flooded by liquid, the β_v of the two CCs should be 0.5 in this orientation. In the horizontal orientation, however, the liquid will prefer to stay at the bottom of the two CCs and the liquid core due to gravity. The liquid-vapor interface must be at least tangent to the top of the liquid core which is filled with liquid, as shown in Fig. 5. The area of the CC section that is not liquid filled, $A_{\text{vap,CC}}$, can be obtained, as shown in Eq. (3).

$$A_{\text{vap,CC}} = \pi R_{\text{CC}}^2 \times \frac{\pi - 2\sin^{-1}(R_{\text{LC}}/R_{\text{CC}})}{2\pi} - R_{\text{LC}}\sqrt{R_{\text{CC}}^2 - R_{\text{LC}}^2} \quad (3)$$

The volume percentage of the two CCs that are liquid filled, β_h, in the horizontal orientation can be written as Eq. (4),

$$\beta_h = 1 - \frac{A_{\text{vap,CC}}}{A_{\text{CC}}} = 1 - \frac{\pi R_{\text{CC}}^2 \times [\pi - 2\sin^{-1}(R_{\text{LC}}/R_{\text{CC}})/2\pi] - R_{\text{LC}}\sqrt{R_{\text{CC}}^2 - R_{\text{LC}}^2}}{\pi R_{\text{CC}}^2} \quad (4)$$

As shown in Fig. 5, when the liquid floods the liquid core in the horizontal orientation, the area of the CC section that is not liquid filled, $A_{\text{vap,CC}}$, is always less than half of the CC section area, A_{CC}, namely, the value of β_h in the horizontal orientation is always greater than 0.5. Comparing the values of the two fill factors for the two typical orientations, namely, β_h and β_v, the larger one β_h should be chosen to satisfy the modified cold condition at any orientation. This value can assure that, within a certain temperature range, the DCCLHP will not only be able to start up and operate at any orientation, but also avoid the most difficult startup situation.

C. Test Setup

Heat input to the evaporator was provided by film heaters, which were attached directly on the evaporator symmetrically. The heat load can be controlled by the input voltage. The condenser line was mounted on an aluminum cold plate with imbedded coolant channels, which was cooled by a low constant temperature trough. Because the liquid and vapor lines were flexible stainless steel tube, the different orientations of the evaporator, the CC, and the condenser were easy to obtain in the tests. The entire loop was thermally insulated with sponge, which had the thermal resistance of about 10 K/W per unit length, to reduce the parasitic heat loss.

For the convenience of description, the CC without the bayonet inside was defined as CC 1, whereas the CC with the bayonet inside was defined as CC 2. 20 copper/constantan (type T) thermocouples (TCs), used to monitor the temperature profiles of the loop. The data acquisition system which consisted of a data logger linked to a PC and the IMPview software was used to display and save the data. Figure 6 shows the thermocouple locations. In the horizontal orientation, TC 1 was located on the top of the CC 1 away from the evaporator, whereas TC 2 was located on the bottom of CC 1 near the evaporator. TC 7 was located on the top of the CC 2 away from the evaporator, whereas TC 8 was located on the bottom of the CC 2 near the evaporator. TCs 3, 4, and 5 were on the evaporator shell. TC 6 was at the evaporator outlet, namely, the vapor line inlet, and TC 9 was at the CC 2 inlet, namely, the liquid line outlet. TC 10 was for the ambient temperature. TC 13 and TC 17 were, respectively, at the condenser inlet and outlet. TC 14, TC 15, and TC 16 divide the condenser line into four with the distance of about 500 mm. The TCs on the vapor and liquid lines were spaced out 500 mm apart.

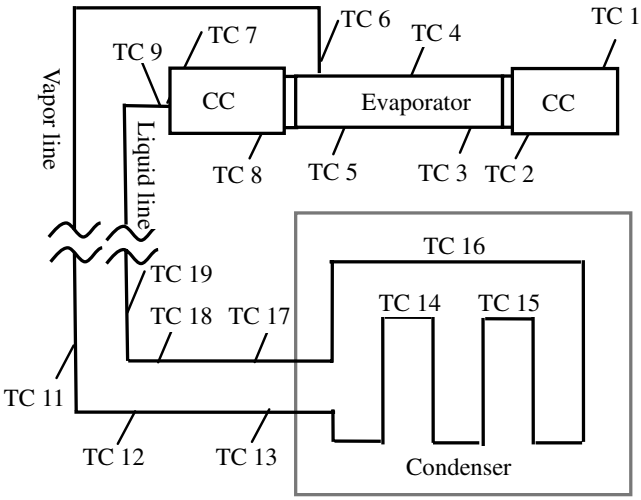

Fig. 6 DCCLHP schematic with thermocouple locations.

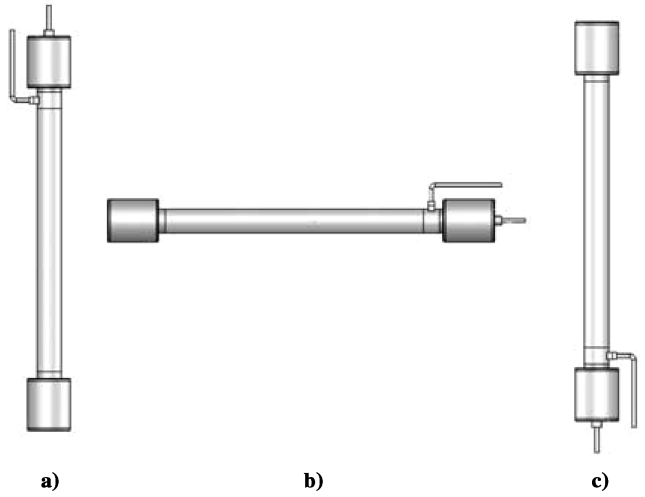

Fig. 7 Three orientations of evaporator and CCs: a) vertical I, b) horizontal, and c) vertical II.

In this paper, the operational characteristics of the DCCLHP are to be investigated at different orientations between the evaporator and the CCs. The three typical orientations are shown in Fig. 7. As the ability of the LHPs to operate at adverse elevations has already been validated, all the tests were conducted without adverse elevations except for the startup tests.

III. Test Results and Discussion

A. Startup Characteristics

The working fluid charge mass and the CC volume of the test DCCLHP were concurrently designed to flood the liquid core with liquid at any orientation to reduce the heat leak from the evaporator to the CC and avoid the most difficult startup situation. For a conventional LHP, there are four startup situations depending on the liquid-vapor composition in the liquid core and the vapor grooves. However, if the liquid core of the DCCLHP was always flooded by liquid, namely, if the concurrent design was successful and effective, only two startup situations would appear: the situation that liquid floods the vapor grooves and the situation that vapor exists in the vapor grooves.

The most unfavorable vapor/liquid distribution in the loop for startups, namely, liquid floods the vapor grooves whereas vapor exists in the liquid core, was expected to be obtained to investigate the startup performance of the DCCLHP. In the tests, the DCCLHP was at a 0.5-m adverse elevation with the evaporator above the condenser. In this orientation, liquid would prefer to stay in the external loop rather than in the evaporator and the CCs. Because liquid would prefer to flood the bottom CC and the liquid core in the vertical orientation due to the gravity, the startup would be easy. Vapor would exist only in the horizontal orientation if it does exist. Therefore, the horizontal orientation of the evaporator and the CCs at an adverse elevation will provide the most unfavorable vapor/liquid distribution for the startup. If the most difficult startup situation does not occur in this orientation, it will not occur at any other orientation. In such an orientation, more than 40 startup tests were conducted. The test results indicate that there are only two startup situations for the DCCLHP and the most difficult startup like the situation shown in Fig. 3 never occurred. The temperature profiles of the two startup situations of the DCCLHP are shown in Figs. 8 and 9.

In startup situation I shown in Fig. 8, as the heat was applied to the evaporator, the temperature of TC 6 on the evaporator outlet rose with TC 5 on the evaporator, indicating that vapor was generated in the vapor grooves immediately. The temperature rise of TC 13 at the condenser inlet and the temperature drop at the condenser outlet indicate that the loop started to circulate. This startup was very easy. Note that the saturated temperature difference between TC 5 on the evaporator and TC 1/7 on the vapor zone of the CCs was small. This

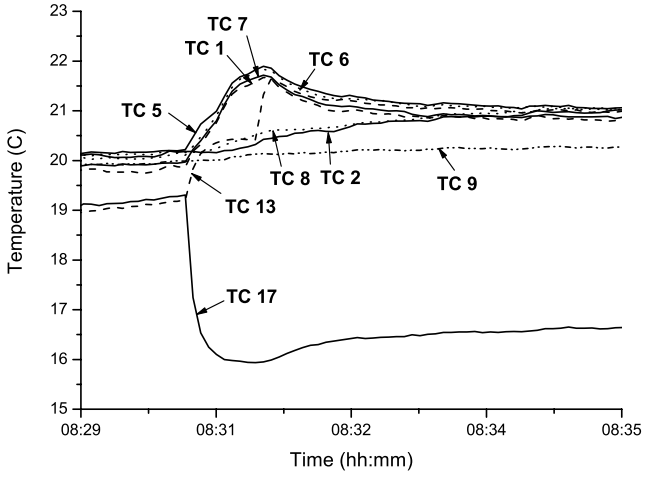

Fig. 8 Startup situation I of the DCCLHP.

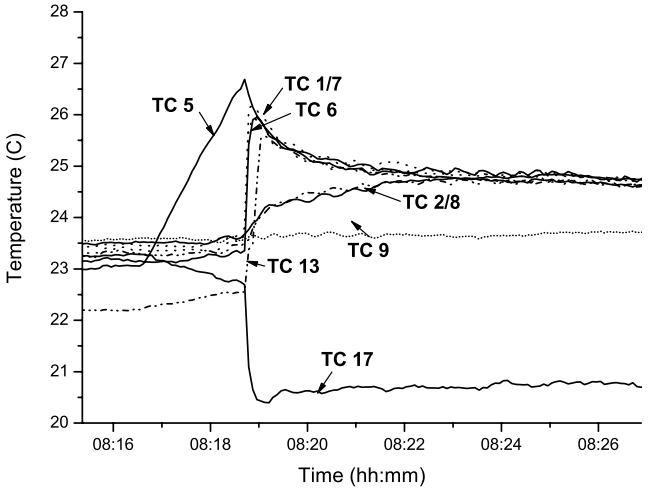

Fig. 9 Startup situation II of the DCCLHP.

is not caused by the high heat leak from the evaporator to the CCs like the startup situation shown in Fig. 2. In the startup in Fig. 2, the temperature of TC CC 2 on the liquid zone rises with TC CC 1, whereas in Fig. 8, TCs 2 and 8 on the liquid zone of the CCs did not rise with TCs 1 and 7 on the vapor zone. The reason for these small temperature differences between the evaporator and the vapor zones on the CCs is that they were all saturated, and the temperature difference between them is related to the pressure difference in accordance with the *Clausis–Clapeyron* relation, namely, Eq. (5).

$$\Delta p = \frac{h_{\mathrm{fg}}}{T_{\mathrm{sat}} v_{\mathrm{fg}}} \Delta T \tag{5}$$

In startup situation II shown in Fig. 9, after the heat was applied on the evaporator, the temperature of TC 6 at the evaporator outlet remained constant and did not rise with the TC 5 on the evaporator, indicating that the vapor grooves had been flooded by liquid before the startup and the nucleate boiling in the vapor grooves required a liquid superheat. When TC 5 on the evaporator kept rising, all the TCs on the two CCs remained constant, indicating that the heat leak from the evaporator to the CCs was small and the liquid core should have been flooded by liquid. Otherwise, the link of the liquid core and the CCs like a conventional heat pipe would have led to the obvious temperature rise of the CCs due to the existence of vapor and the temperature differences between the evaporator and the CCs would have been small like the situation shown in Fig. 3. When the temperature difference between the evaporator and the vapor zone of the CCs, namely, the liquid superheat, was obtained, the nucleate boiling took place immediately and the working fluid started to circulate.

Test results indicate that even when the external loop and the vapor grooves were filled with liquid, the liquid core was still flooded by liquid and the most difficult startup situation never occurred. In the processes of the two startup situations of the DCCLHP, the temperature overshoots of the evaporator were small, the startup times were small, and the startups were easy. Test results indicate that the startup problem of the DCCLHP in gravity can be solved by the concurrent design of the working fluid charge mass and the CC volumes.

B. Operation and Thermal Control Characteristics

For a conventional LHP, there are two modes over the heat load range, namely, the variable conductance mode and the constant conductance mode. When the condenser is not fully utilized and the CC is not flooded by the liquid, the LHP will operate under a variable conductance mode. In this heat load region, the vapor grooves, the condenser, and the CC are all in the two-phase saturated state. According to Eq. (5), as the pressure differences between the three components are limited, the temperature differences between them are very small. Therefore, any of the three temperatures can be considered as the LHP operating temperature. When the CC is in a saturated state under the variable conductance mode, the operating temperatures can be controlled within a very narrow range by actively applying a small additional heat load to the CC to maintain its saturated temperature, which is one of the important characteristics of the LHP. As the heat load on the evaporator increases and reaches a certain value, the liquid in the condenser will be pushed to the CC. When the condenser is fully utilized and the CC is fully filled by liquid, the LHP will operate under a constant conductance mode. In this heat load region, the saturated temperatures of the evaporator and the condenser can be considered as the operating temperature, whereas the CC is in the subcooled state. The operating temperatures of the LHP cannot be controlled by actively maintaining the CC temperature.

Although the DCCLHP also has the same two modes over the heat load range, as the vapor/liquid distributions in the two CCs are different at various orientations, the operation and thermal control characteristics will be different from the conventional LHP. Because the thermal equilibriums in the CCs directly affect the operation and thermal control of the DCCLHP, the temperature profiles on the two CCs must be carefully noted.

1. *Horizontal Orientation*

Figures 10 and 11 show the component temperature profiles at various heat loads in the horizontal orientation. On the abscissa in Figs. 10, temperatures are, respectively, measured by TCs 1 and 2 on the CC 1, TC 5 on the evaporator, TC 6 at the vapor inlet, TC 13 to TC 17 on the condenser line, TCs 18 and 19 on the liquid line, TC 9 at the CC inlet, and TCs 7 and 8 on the CC 2.

Note that, in the horizontal orientation shown in Fig. 7b, when the LHP operated under the variable conductance mode, TC 1 and TC 7 on the top of the two CCs were measuring the local vapor temperatures whereas TC 2 and TC 8 on the bottom of the two CCs were measuring the local liquid temperatures. When the LHP operated under the constant conductance mode, the four TCs on the two CCs were all measuring the local liquid temperatures.

At 50 W, as shown in Fig. 10, the temperatures of TCs 1 and 7 on the vapor zone of the two CCs were close to the saturated temperatures of TC 5 on the evaporator and TC 13 at the condenser inlet, indicating that the two CCs were both in the saturated state. Therefore, the DCCLHP was under the variable conductance mode and the operating temperatures could be controlled within a narrow range by applying additional heat loads to any of the two CCs. As with the conventional LHP, the generated vapor flew from the vapor grooves to the vapor line and then was condensed to liquid and

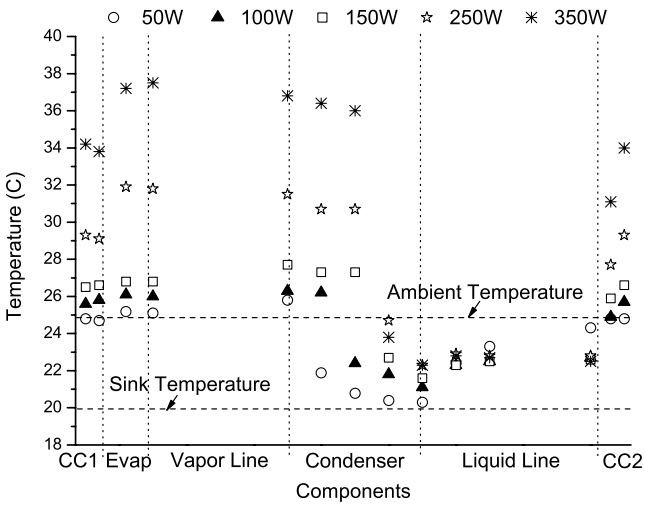

Fig. 10 Temperature profiles of components in the horizontal orientation.

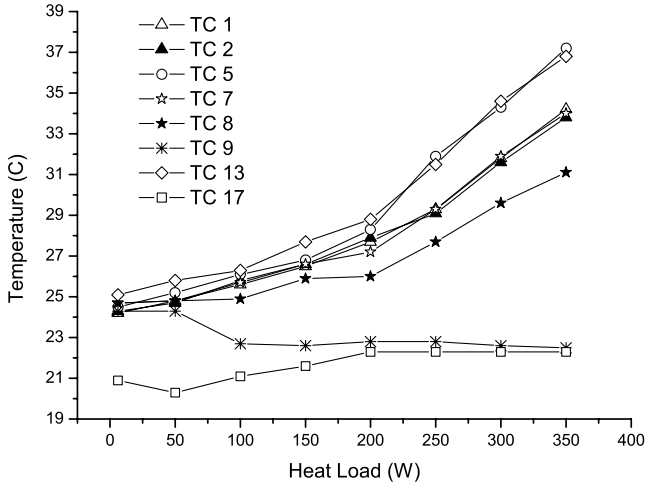

Fig. 11 Temperatures versus heat load in horizontal orientation.

subcooled at TC 14. The liquid working fluid was close to the sink temperature when they flowed to the condenser outlet of TC 17. Because the liquid line was not absolutely thermally insulated and the flow rate of the fluid was small at low heat loads, the return liquid was heated by the ambience. The liquid temperature rose to near the ambient temperature as they enter the CC. When the heat loads were below 50 W, as the two CCs were both in the two-phase saturated state, the temperature difference between TC 1 and TC 7 was small. Furthermore, because both the subcooling degree and the mass flow rate of the return liquid were small, the return subcooled liquid had little effect on the temperature profiles of the CCs. As shown in Fig. 11, at equilibrium, the four TCs on the two CCs were all close to the saturated temperature and their temperature differences were very small.

When the heat loads were increased to 100 and 150 W, the temperatures of TCs 1 and 7 on the CCs were still close to the saturated temperatures, indicating that the DCCLHP was still operating under the variable conductance mode and the operating temperatures could be controlled by applying heat loads to any CC. At equilibrium, the two-phase heat transfer area increased in the condenser, indicated by the sharp temperature rise of TC 14 and TC 15. As the subcooled zone decreased and the mass flow rate increased, TC 17 at the condenser outlet rose. However, because the increased flow rate decreased the effect of the heat loss from ambience, the subcooling of the return liquid at the liquid line outlet finally increased. As shown in Fig. 11, the subcooling degree of TC 9 at the CC inlet increased to 3.4 and 4.2°, respectively, at 100 and 150 W. Because of the increases in both the liquid subcooling and the mass flow rate, the heat transfer between the return liquid in the bayonet and the fluid in the CC 2 was enhanced. Because of the natural convection of the working fluid outside the bayonet in the CC 2, TC 8 of the liquid zone at the CC 2 bottom was subcooled and its temperature was lower than TC 7 of the vapor zone on the CC 2 top. As the two CCs were both in a saturated state, according to Eq. (5), the saturated vapor temperature of TC 1 on the CC 1 was close to TC 7 on the CC 2. As no bayonet existed in the CC 1, the temperature difference between TC 1 on the top and TC 2 at the bottom was small, as shown in Fig. 11.

When the heat loads were increased to 250 and 350 W, the four TCs on the two CCs were lower than the saturated temperature, indicating that both the CCs were flooded by subcooled liquid and the condenser was fully utilized. In this heat load region, the DCCLHP was operating under the constant conductance mode and the operating temperatures could not be controlled by applying heat loads to the CCs. As shown in Fig. 11, the temperature differences between TC 5 on the evaporator and TC 1 or TC 7 on the CCs, namely, the subcooling degrees of the CCs, were 2.6 and 3.2°, respectively, at 250 and 350 W. As the heat load was increased, the temperature difference between TC 7 on the top and TC 8 at the bottom increased for the existence of the bayonet inside the CC 2.

2. Vertical Orientation I

Figures 12 and 13 show the component temperature profiles at various heat loads in the vertical orientation I (the CC 2 with the bayonet inside was on the top). Note that, in the vertical orientation I shown in Fig. 7a, when the LHP operated under the variable conductance mode, TC 8 on the end of the CC 2 away the evaporator was measuring the local vapor temperatures, whereas TCs 1, 2, and 7 on the CCs were all measuring the local liquid temperatures. When the LHP operated under the constant conductance mode, the four TCs on the two CCs were all measuring the local liquid temperatures.

At 50 W, as shown in Fig. 12, only the CC 2 above the evaporator was in the saturated state, indicating that the DCCLHP was operating under the variable conductance and the operating temperatures could only be controlled by applying heat load to the CC 2. As the CC 1 below the evaporator was flooded by liquid, although the temperature difference between the two CCs was small, applying heat load to CC 1 could not realize the operating temperature control. Similar to the situation in the horizontal orientation, because the subcooling of the return liquid was very small at low heat load, it had little effect on the temperature profiles of the CCs. As shown in Fig. 13, the temperature differences between the four TCs on the two CCs were small.

When the heat loads were increased to 100 and 150 W, the above CC 2 was still in the saturated state and the DCCLHP was operating under the variable conductance mode. As the CC 1 below the evaporator was liquid filled and subcooled, only applying heat load on the CC 2 could realize the operating temperature control. Because the CC 2 and the evaporator were both in the saturated state, the

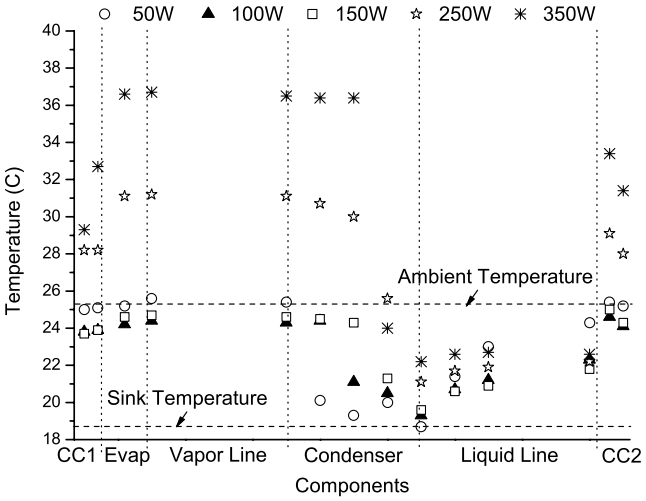

Fig. 12 Temperature profiles of components in vertical orientation I.

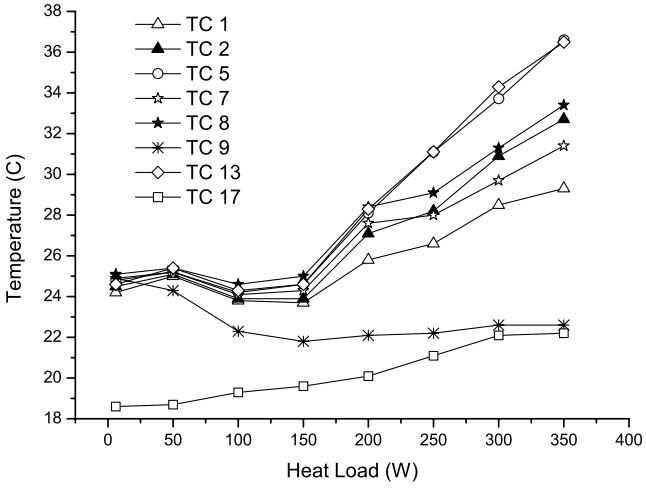

Fig. 13 Temperatures versus heat load in vertical orientation I.

temperature difference between TC 7 on the vapor zone and TC 5 was small, shown in Fig. 13. Because of the natural convection (or buoyancy effect) in the CC 1 and the liquid core, the CC 1 below the evaporator was cooled, and both TCs 1 and 2 were subcooled. The subcoolings of these two TCs on the CC 1 were small, and the temperature of TC 1 was lower than TC 2.

When the heat loads were increased to 250 and 350 W, the two CCs were both flooded by liquid and subcooled and the DCCLHP was operating under the constant conductance mode. In this heat load region, the operating temperature control could not be realized by applying heat load to the CCs. The cooling effect of the return liquid on the CCs was enhanced for the increased subcooling of the return liquid. As shown in Fig. 13, the temperature of TC 1 at the bottom of the CC 1 below the evaporator was the lowest among the four TCs on the CCs due to the natural convection. The temperature of TC 7 on the above CC 2 was lower than TC 2, because the above CC 2 was cooled by the return liquid in the bayonet.

3. Vertical Orientation II

Figures 14 and 15 show the component temperature profiles at various heat loads in the vertical orientation II (the CC 2 with the bayonet inside was at the bottom). Note that, in the vertical orientation I shown in Fig. 7c, when the LHP operated under the variable conductance mode, TC 1 on the end of the CC 1 away from the evaporator was measuring the local vapor temperatures, whereas TCs 2, 7, and 8 on the CCs were all measuring the local liquid temperatures. When the LHP operated under the constant conductance mode, the four TCs on the two CCs were all measuring the local liquid temperatures.

At 50 W, as shown in Fig. 14, only the CC 1 above the evaporator was in the saturated state, indicating that the DCCLHP was operating under the variable conductance. As the CC 2 below the evaporator was flooded by liquid, only applying heat load on the CC 1 could realize the operating temperature control. Because the subcooling of the return liquid was very small at low heat load, it had little effect on the temperature profiles of the CCs. As shown in Fig. 15, the temperature differences between the four TCs on the two CCs were small.

When the heat loads were increased to 100 and 150 W, the above CC 1 was still in the saturated state and the DCCLHP was operating under the variable conductance mode. Because the CC 2 below the evaporator was liquid filled and subcooled, only applying heat load on the CC 1 could realize the operating temperature control of the DCCLHP. As the CC 1 and the evaporator were both in the saturated state, the temperature differences between TC 1, TC 2 on the CC 1, and TC 5 were small, as shown in Fig. 15. Because of the natural convection and the cold bayonet inside the CC 2, the CC 2 below the evaporator was deeply subcooled (the subcooled temperature of TC 7 on the CC 2 end away from the evaporator was 7.1° at 150 W). The temperature of TC 8 on the CC 2 end near the evaporator was higher than TC 7 for the heat leak from the evaporator.

Note that, in the vertical orientation II, the heat load region under the variable conductance mode was extended. As shown in Fig. 15, CC 1 was still in the saturated state at 250 W, whereas it was already subcooled in both the horizontal orientation and the vertical orientation I. In the vertical orientation II shown in Fig. 14, TCs 13 and 14 were saturated, whereas TC 15 was still subcooled at 250 W. TC 15 rose to the saturated temperature until the heat load was increased to 350 W. However, in the horizontal orientation and the vertical orientation I, TC 15 already rose to the saturated temperature at 150 W. The results indicated that the heat load required to push the vapor/liquid interface to the point of TC 15 in the condenser was less than 150 W in the horizontal orientation and the vertical orientation I, whereas it was about 350 W in the vertical orientation II. As the condenser was not fully utilized in the vertical orientation II at 250 W, the above CC 1 was not flooded by liquid and was still in the saturated state. The heat load region of the variable conductance mode was from 0 W to more than 250 W, whereas it was from 0 to 200 W in the other two orientations. The extended heat load region of the variable conductance in the vertical orientation II was caused by

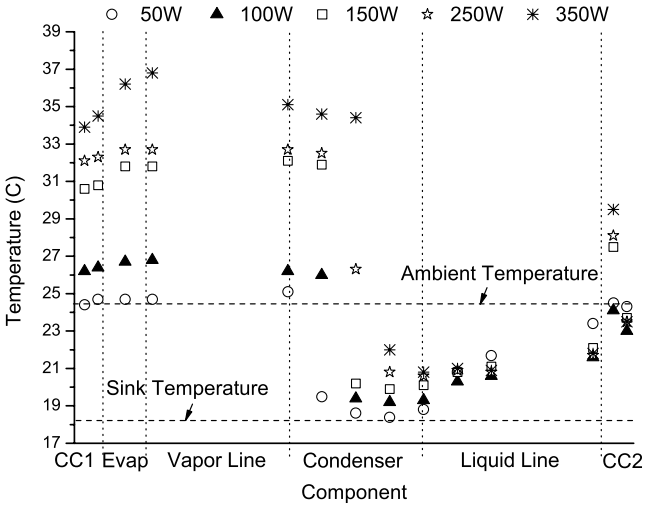

Fig. 14 Temperature profiles of components in vertical orientation II.

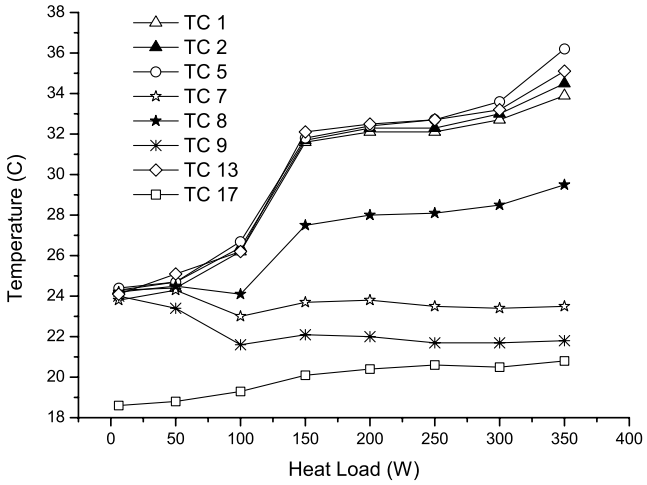

Fig. 15 Temperatures versus heat load in vertical orientation II.

the thermal equilibrium changes in the saturated CC 1. Because most of the subcooling of the return liquid was used to cool the CC 2 instead of the CC 1 in the vertical orientation II, the heat leak from the evaporator to the CC 1 led to the higher saturated temperature rise in the CC 1 than in the other two orientations. According to Eq. (5), a higher saturated temperature in the vapor grooves, which can be obtained by a higher heat load on the evaporator, was required to push the liquid in the condenser to the CC 1. This was the reason that the heat load region of the variable conductance mode was extended in the vertical orientation II.

When the heat loads were increased to 300 and 350 W, the two CCs were flooded by liquid and subcooled and the DCCLHP was operating under the constant conductance mode. The cooling effect of the return liquid on the CC 2 was enhanced as the subcooling of the return liquid increased. Because of the natural convection and the cold bayonet in the CC 2, the subcooled degree of TC 7 already increased to 12.7° at 350 W, as shown in Fig. 15. The TCs 1 and 2 on the CC 1 also got a little subcooled, and TC 2 was higher than TC 1 for the heat leak from the evaporator.

Then, the operation and thermal control characteristics of the DCCLHP in different orientations can be summarized as shown in Table 2.

D. Effect of Orientation on Operating Temperatures

Although the DCCLHP could start up easily and operate normally in any orientation, test results indicated that, in the certain heat load region, the final steady-state operating temperatures of the DCCLHP

Table 2 Operation and thermal control characteristics of the DCCLH

Item	Horizontal	Vertical I	Vertical II
Heat load range of variable conductance mode	0–200 W	0–200 W	0–250 W
Which CC can realize the temperature control	Any of the CCs	The above CC 2	The above CC 1
State of the two CCs at high heat loads under variable conductance mode	CC 1: saturated CC 2: saturated	CC 1: slightly subcooled CC 2: saturated.	CC 1: saturated CC 2: deeply subcooled

were not the same in the three different orientations. Figures 16 and 17 show the operating temperature and thermal conductance at various heat loads. The thermal conductance of the DCCLHP is defined as Eq. (6),

$$G = \frac{Q}{(T_{\text{evap}} - T_{\text{sink}})} \tag{6}$$

As Table 2 shows, the heat load region of the variable conductance in the horizontal orientation and the vertical orientation I was from 0–200 W, whereas it was from 0–250 W in the vertical orientation II. When the heat load was more than 300 W, the DCCLHP was operating under the constant conductance mode in any orientation. As shown in Fig. 16, the DCCLHP operating temperatures in the three orientations are close to each other in both the lower heat load region under the variable conductance mode (less than 50 W) and the heat load region under the constant conductance mode (more than 300 W). The operating temperature differences in the different orientations appear in the higher heat load region under the variable conductance mode (from more than 75 to 200 W). The operating temperatures in the vertical orientation I are the highest, and those in the vertical orientation II are the lowest.

As the DCCLHP operating temperatures under the variable conductance mode were determined by the thermal equilibrium in the saturated CC, the thermal analysis in the saturated CC can explain the operating temperature difference in the three orientations.

In vertical orientation I, the operating temperatures under the variable conductance mode were determined by the thermal equilibrium in the saturated CC 2, which had the bayonet inside. At equilibrium, the evaporating mass rate on the outside surface of the primary wick would be equal to the mass flow of the return liquid into the liquid core. Therefore, the vapor/liquid interface in the CC 2 would not change (neither rise nor drop), namely, no liquid would flow into or out of the saturated CC 2. As shown in Fig. 18, the heat transfers which affect the thermal equilibrium in the CC 2 are those: the axial heat leak from the evaporator to the CC 2 through the primary wick, $Q_{\text{HL,CC 2}}$; the heat transfer between the liquid fluid in the liquid core and the CC 2, $Q_{\text{CC 2-LC}}$, which is positive if heat is transferred from the liquid core to the CC 2 and negative if heat is transferred in the reverse direction; the heat transfer between the fluid in the CC 2 and the cold return liquid in the bayonet by the mode of fluid convection and bayonet conduction, $Q_{\text{CC 2-bay}}$; and the heat transfer between the CC 2 and the ambience, $Q_{\text{CC 2-amb}}$, which is positive if heat is transferred from ambience to the CC and negative if heat is transferred in the reverse direction. The energy equilibrium in the CC 2 can be written as Eq. (7),

$$\Delta E_{\text{CC 2}} = Q_{\text{HL,CC 2}} + Q_{\text{CC 2-LC}} - Q_{\text{CC 2-bay}} \tag{7}$$

In the vertical orientation II, the operating temperatures under the variable conductance mode were decided by the thermal equilibrium in the saturated CC 1. As no bayonet is inside of the CC 1, the term of the heat transfer between the fluid in the CC 2 and the cold return liquid in the bayonet, $Q_{\text{CC 2-bay}}$, does not exist. Therefore, the energy equilibrium in the CC 2 can be written as Eq. (8),

$$\Delta E_{\text{CC 1}} = Q_{\text{HL,CC 1}} + Q_{\text{CC 1-LC}} + Q_{\text{CC 1-amb}} \tag{8}$$

In the horizontal orientation, although the thermal boundary conditions in the two CCs are different, as the saturated temperature difference between the two CCs is related to their pressure difference in accordance with the Clausis–Clapeyron relation, the thermal equilibrium between the two CCs will affect each other. Therefore, the operating temperature of the DCCLHP will be decided by the two CCs together. In a simplified analysis, the two CCs can be considered

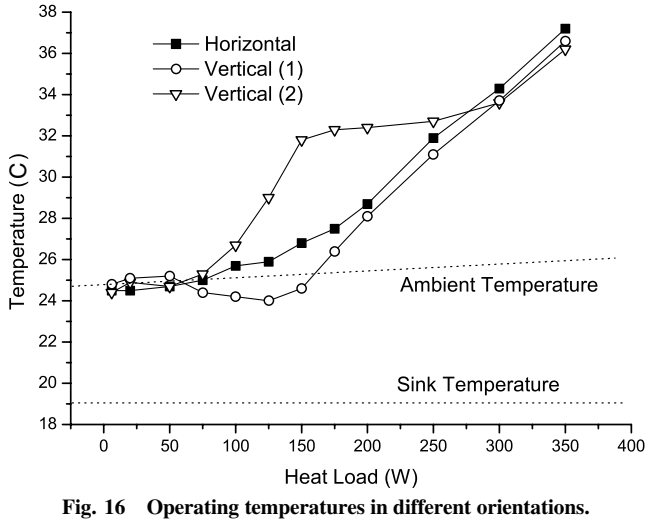

Fig. 16 Operating temperatures in different orientations.

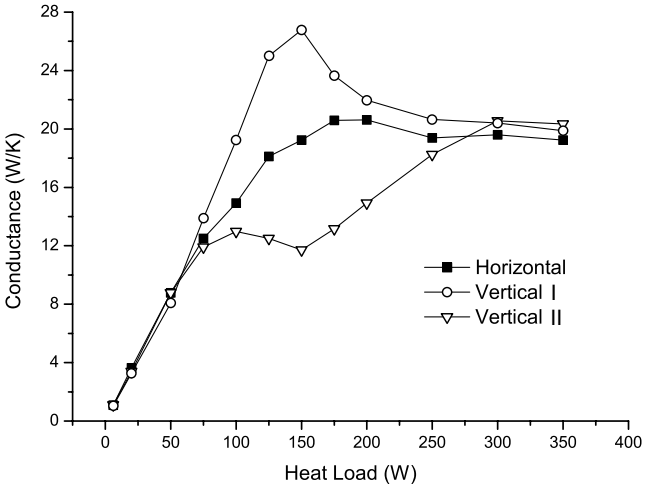

Fig. 17 Conductance in different orientations.

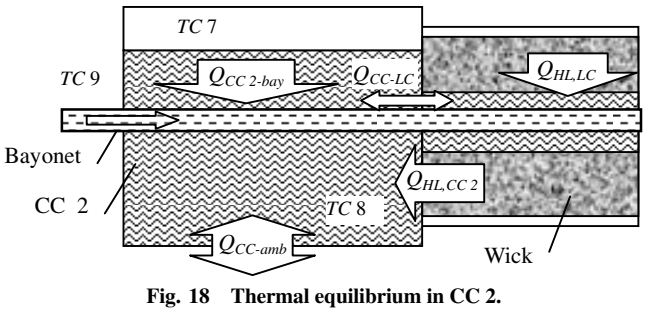

Fig. 18 Thermal equilibrium in CC 2.

as an integrated one. The energy equilibrium can be written as Eq. (9),

$$\Delta E_{CC} = Q_{HL,CC\,1} + Q_{HL,CC\,2} + Q_{CC\,1\text{-}LC} + Q_{CC\,2\text{-}LC} + Q_{CC\,1\text{-}amb} + Q_{CC\,2\text{-}amb} - Q_{CC\,2\text{-}bay} \quad (9)$$

As the entire loop was thermally insulated with the sponge to reduce the heat transfer between the components and the ambience in the tests, the term of $Q_{CC\,2\text{-}amb}$ is small. Moreover, as the thermal conductivity of the liquid fluid is very low, the term of the heat transfer between the liquid fluid in the liquid core and the CC, $Q_{CC\text{-}LC}$, is also very small. Ignoring the terms of $Q_{CC\,2\text{-}amb}$ and$Q_{CC\text{-}LC}$, the two main factors that affect the thermal equilibrium of the DCCLHP are the axial heat leak from the evaporator to the CC through the primary wick, $Q_{HL,CC}$, and the heat transfer between the fluid in the CC 2 and the cold return liquid in the bayonet, $Q_{CC\,2\text{-}bay}$. Obviously, a larger $Q_{CC\,2\text{-}bay}$ is preferred for the DCCLHP to operate at a lower operating temperature.

At low heat loads (less than 50 W), as the subcooling of the return liquid that flows into the bayonet inside the CC 2 is very small due to the low mass flow rate at low heat loads, the heat transfer between the fluid in the CC 2 and the cold return liquid in the bayonet is very small. The axial heat leak from the evaporator to the saturated CC, $Q_{HL,CC}$, is also small at low heat loads. Therefore, the existence of the bayonet inside the CC has little effect on the thermal equilibrium in the CC, and the operating temperatures in the three different orientations are close to each other. As the heat loads increase (75–250 W), the mass flow rate and the subcooling of the return liquid increase, and the heat transfer between the fluid in the CC 2 and the cold return liquid in the bayonet,$Q_{CC\,2\text{-}bay}$, is enhanced. If the bayonet is inside the above CC, namely, in the vertical orientation I, as shown in Eq. (7), the existence of $Q_{CC\text{-}bay}$ will lead to lower saturated temperatures in the CC at equilibrium. If no bayonet is inside the above CC, namely, in the vertical orientation II, as shown in Eq. (8), the term of $Q_{CC\text{-}bay}$ does not exist. As the subcooled return liquid cannot cool the above saturated CC, the saturated temperatures will be higher at equilibrium. In the horizontal orientation, as shown in Eq. (9), the term of $Q_{CC\text{-}bay}$ does exist, but two heat leaks to the two saturated CCs, namely, $Q_{HL,CC\,1}$ and $Q_{HL,CC\,2}$, are to be balanced, so that the saturated temperatures in the horizontal orientation are higher than those in the vertical orientation I and lower than those in the vertical orientation II. At high heat loads (more than 300 W), the DCCLHP operates under the constant conductance mode and the CCs are in the subcooled state. In this heat load region, the operating temperatures under the constant conductance mode are decided by the effective two-phase heat transfer area in the condenser instead of the thermal equilibrium in the CCs. The heat transfer between the fluid in the CC and in the bayonet cannot affect the operating temperatures of the DCCLHP much. Therefore, the operating temperatures in the three orientations are close to each other again in this heat load region.

Besides the above thermal equilibrium analysis in the saturated CC, the operating temperature differences of the DCCLHP in the certain heat load region can also be explained by the different usage efficiency of the subcooling of the return liquid in the three orientations. For the convenience of describing, the subscript of CC is used to denote the CC in the saturated state, on which applying heat load can realize the active operating temperature control. CC′ is used to denote the liquid-filled CC, on which applying heat load cannot realize the active operating temperature control.

The subcooling of the return liquid at the CC inlet, Q_{sub}, can be classified into three parts, as shown in Eq. (10): the part to offset the axial heat leak from the evaporator to the CCs across the primary wick, $Q_{HL,CC'}$ and $Q_{HL,CC}$; the part to offset the radial heat leak from the evaporator to the liquid core across the primary wick, $Q_{HL,LC}$; and the part to cool the liquid fluid in the liquid core and the CCs to be subcooled, $Q_{sub,sub}$.

$$Q_{sub} = Q_{HL,CC} + Q_{HL,CC'} + Q_{sub,sub} \quad (10)$$

According to the effect of subcooling on the saturated temperature or thermal equilibrium in the saturated CC, which can realize the operating temperature control, the return liquid subcooling can also be classified into two parts, namely, the effective part and the ineffective part. The part of the return liquid subcooling that offset the axial heat leak from the evaporator to the saturated CC that can realize the operating temperature control, $Q_{HL,CC}$, is obviously effective. This part can affect the thermal equilibrium in the saturated CC and the operating temperature of the DCCLHP. The part of the return liquid subcooling that cools the liquid fluid in the liquid core and the CCs to be subcooled, $Q_{sub,sub}$, is obviously ineffective, because the subcooled liquid in the liquid core and the CCs cannot decrease the saturated temperature (affect the thermal equilibrium) in the saturated CC. However, the part of the return liquid subcooling that offset the axial heat leak from the evaporator to the liquid-filled CC that cannot realize the operating temperature control, $Q_{HL,CC'}$, and the radial heat leak from the evaporator to the liquid core, $Q_{HL,LC}$, cannot affect the saturated temperature or equilibrium in the saturated CC directly. It can, however, affect the thermal equilibrium in the liquid core and the liquid-filled CC, which are thermally linked to the saturated CC. Therefore, this part can indirectly affect the saturated temperature in the saturated CC. Although the effect of this part of the return liquid subcooling on the thermal equilibrium in the saturated CC is difficult to accurately quantify, two factors with a value from 0 to 1 can be used in the discussion. Then, the effective subcooling of the return liquid can be written as Eq. (11), where $\chi_{HL,LC}$ and $\chi_{HL,CC'}$ denote the two parts of the return liquid subcooling which offset $Q_{HL,LC}$ and $Q_{HL,CC}$, respectively,

$$Q_{sub,eff} = Q_{HL,CC} + \chi_{HL,CC'} Q_{HL,CC'} + \chi_{HL,LC} Q_{HL,LC} \quad (11)$$

Now, the effective usage efficiency of the return liquid subcooling, namely, the ratio of the effective or useful part, which can cool the saturated CC, to the total return liquid subcooling at the CC inlet can be defined as Eq. (12). Obviously, a higher usage efficiency of the return liquid subcooling is preferred for a lower operating temperature or thermal resistance of the DCCLHP.

$$\eta = \frac{Q_{sub,eff}}{Q_{sub}} = \frac{Q_{sub,eff}}{\dot{m} c_{p,l} \Delta T_{sub}} = \frac{Q_{HL,CC} + \chi_{HL,CC'} Q_{HL,CC'} + \chi_{HL,LC} Q_{HL,LC}}{Q_{HL,CC} + Q_{HL,CC'} + Q_{HL,LC} + Q_{sub,sub}} \quad (12)$$

When the above CC has the bayonet inside, namely, in the vertical orientation I, as shown in Fig. 13, in the heat load region from 75 to 250 W, the temperatures of TC 8 on the liquid zone and TC 7 on the liquid zone of the CC 2 with the bayonet inside were both saturated. TCs 1 and 2 on the bottom CC 1 were only a little subcooled, indicating that most of the return liquid subcooling had offset the heat leak from the evaporator to the saturated CC 2 to lower the operating temperature of the DCCLHP. The subcooled return liquid had offset the axial heat leak from the evaporator, $Q_{HL,CC}$, to cool the fluid in the saturated CC 2 when it flowed through the CC 2 in the bayonet. This offset the radial heat leak from the evaporator to the liquid core across the primary wick, $Q_{HL,LC}$, and the axial heat leak from the evaporator to the liquid-filled CC 1, $Q_{HL,CC'}$, when it flowed into the liquid core. The liquid in the CCs and the liquid core was not remarkably subcooled by the return cold liquid. The usage efficiency of the return liquid subcooling in this orientation was high.

When the CC 2 with a bayonet inside was below the evaporator, namely, in the vertical orientation II, as shown in Fig. 15, in the heat load region from 75 to 250 W, TC 1 on the liquid zone and TC 2 on the liquid zone of the CC 1 were both near the saturated temperature. However, TCs 7 and 8 on the bottom CC 2 with the bayonet inside were deeply subcooled (the temperature difference between TC 1 and TC 7 or 8 was large), indicating that part of the return liquid subcooling had been wasted to cool the fluid in the liquid-filled CC 2 instead of the saturated CC 1. The cold return liquid cooled the CC 2 when it flew through the CC 2 in the bayonet. Besides offsetting the axial heat leak to the liquid-filled CC 2, $Q_{HL,CC'}$, and the radial heat leak from the evaporator to the liquid core, $Q_{HL,CC}$, most of the return

liquid subcooling did not offset the axial heat leak to the saturated CC 1, $Q_{HL,CC}$. Rather, it preserved in the subcooled liquid in the CC 2 and the liquid core, which was ineffective to lower the operating temperature of the DCCLHP. The usage efficiency of the return liquid subcooling in this orientation was low.

In the horizontal orientation, as shown in Fig. 11, in the heat load region from 75 to 250 W, the four TCs on the two CCs were near the saturated temperature. Only TC 8 at the bottom of the CC 2 with the bayonet inside was slightly subcooled, indicating that most of the return liquid subcooling had offset the heat leak to the two saturated CCs. The usage efficiency of the return liquid subcooling in this orientation was also high. However, as the two CCs were all saturated in the horizontal orientation, the factor of $\chi_{HL,CC'}$ in Eqs. (11) and (12) should be equal to 1, and the effective subcooling of the return liquid must offset the axial heat leak to the two CCs.

In conclusion, in the heat load region from 75 to 250 W, the usage efficiency of the return liquid subcooling in the vertical orientation I was high and the operating temperatures of the DCCLHP were lowest. Alternatively, the usage efficiency of the return liquid subcooling in the vertical orientation II was low and the operating temperatures of the DCCLHP were the highest. Although the usage efficiency of the return liquid subcooling in the horizontal orientation was also high, the effective subcooling of the return liquid must offset the heat leak to the two CCs, so that the operating temperatures of the DCCLHP were higher than those in the vertical orientation I and lower than those in the vertical orientation II.

E. Other Results and Suggestions

The above test results and discussion also give a suggestion for the mathematical model of the LHP. The existing mathematical model [6,7] assumed that the liquid core and the CC contained both vapor and liquid (two-phase fluid) at all times and the fluid in the liquid core and the CC was saturated. According to this assumption, the saturated temperature difference between the liquid core and the CC was very small and the energy equilibrium in the saturated CC was considered as the balance of the heat leak from the evaporator to the liquid core across the wick and the whole subcooling of the return liquid at the CC inlet, as written in Eq. (13). The test results and analysis of the DCCLHP in this paper indicate that not all the subcooling of the return liquid has offset the heat leak to the saturated CC. Actually, part of the return liquid subcooling cooled the liquid to be locally subcooled. The part wasted in cooling the liquid to be subcooled should be considered in the mathematical modeling. Therefore, the thermal equilibrium in the saturated CC should be considered as the balance of the heat leak from the evaporator to the saturated CC and the effective subcooling of the return liquid, as shown in Eq. (14). The item of $Q_{sub,eff}$ in the Eq. (14) is already explained in Eqs. (11) and (12). The assumption of neglecting the existence of the subcooled liquid in the liquid core and the CC would cause the inaccuracy in the model and the calculated operating temperatures would be lower than the test results. Furthermore, the existing mathematical model cannot explain the phenomena of the operating temperature differences in the three different orientations and other operational characteristics of the DCCLHP. Besides, in the modeling of the DCCLHP, the existence of the bayonet and the fluid flow and heat transfer in the liquid core and the two CCs are important and should be considered.

$$\Delta E_{CC} = Q_{HL,LC} - Q_{sub} \tag{13}$$

$$\Delta E_{CC} = Q_{HL,CC} - Q_{sub,eff} = Q_{HL,CC} - \eta Q_{sub} \tag{14}$$

The above test results and analysis of the DCCLHP also indicate that an effective method to decrease the operating temperature or thermal resistance of the DCCLHP is to increase the usage efficiency of the return liquid subcooling. Measures, such as increasing the heat transfer area by twisting the bayonet inside the saturated CC, can be taken to enhance the heat transfer between the return liquid and the fluid in the saturated CC to increase the usage efficiency of subcooling. Furthermore, another extreme measure is to extend the bayonet just into the saturated CC instead of the liquid core. According to Eqs. (10) and (11), the usage efficiency of the return liquid subcooling is the highest. However, the bayonet into the liquid core was designed to push the gas or bubble out of the liquid core and the measure would have negative effects on the stability of the LHP.

IV. Conclusion

Test results indicate that the DCCLHP can operate and startup normally in any orientation in gravity and the most difficult startup situation can be avoided by the concurrent design of the working fluid charge mass and the CC volumes. The two startup situations of the DCCLHP observed in the tests appeared very easy with small temperature overshoots and short startup times.

As the DCCLHP had two CCs on the ends of the evaporator, the operation and the thermal control characteristics of the DCCLHP are different from the conventional LHP, which have been summarized in Table 2. The heat load range of the variable conductance in the vertical II orientation (the CC with the bayonet inside at the bottom) is 0–250 W, whereas that in the other two orientations is 0–200 W. Any of the two CCs can realize the temperature control by applying heat load on them in the horizontal orientation, whereas only the top CC can do that in the vertical orientations.

Although the DCCLHP can operate in any orientation, the orientation will affect the final steady-state operating temperatures. The operating temperatures of the DCCLHP in the three orientations are close to each other in both the lower heat load region under the variable conductance mode and the heat load region under the constant conductance mode. The operating temperature difference in the different orientations appeared in the higher heat load region under the variable conductance mode. The operating temperatures in the vertical orientation I (the CC with the bayonet inside is on the top) are the highest and those in the vertical orientation II (the CC with the bayonet inside is at the bottom) are the lowest. This was caused by the bayonet inside the CC and can be explained by the different usage efficiency of the return liquid subcooling in the different orientations.

The test results and discussion of the DCCLHP suggest that part of the return liquid subcooling, which has cooled the liquid to be locally subcooled, must be considered in the mathematical modeling of the LHP. The assumption of neglecting the existence of the subcooled liquid in the liquid core and the CC will cause the calculated operating temperatures to be lower than the test results. Another suggestion is that an effective method, which can decrease the operating temperature or thermal resistance of the DCCLHP, is to enhance the heat transfer between the return liquid and the fluid in the saturated CC to increase the usage efficiency of the return liquid subcooling.

Acknowledgment

This project is supported by the Program for New Century Excellent Talents in Universities.

References

[1] Ku, J. T., "Operating Characteristics of Loop Heat Pipes," Society of Automotive Engineers, Paper 1999-01-2007, 1999.

[2] Maidanik Yu. F., Solodovnik N. N., and Fershtater Y. G., "Investigation of Dynamic and Stationary Characteristics of a Loop Heat Pipe," *Proceedings of the 9th IHPC*, May 1995, pp. 1002–1006.

[3] Zhang H. X., Lin G. P., Ding T., Yao W., Shao X. G., Sudakov R.G., and Maidanik Yu. F. "Investigation on Start-up Behaviors of a Loop Heat Pipe," *Journal of Thermophysics and Heat Transfer*, Vol. 19, No. 4, 2005, pp. 509–518.

[4] Gerhart, C., and Gluck, D. F., "Summary of Operating Characteristics of a Dual Compensation Chamber Loop Heat Pipe in Gravity," *Proceedings of the 11th International Heat Pipe Conference*, Japan Association for Heat Pipes and Seikei Univ., Tokyo, Japan, Sept, 1999, pp. 67–68.

[5] Gluck, D. F., Gerhart, C., and Stanley, S., "Characterization of a High Capacity, Dual Compensation Chamber Loop Heat Pipe," *AIP Conference Proceedings*, Vol. 458, No. 1, 1999, pp. 943–948.

[6] Kaya, T., Hoang, T. T., and Ku, J. T., "Mathematical Modeling of Loop Heat Pipes," AIAA Paper 99-0477, Jan. 1999.

[7] Hoang, T. T., and Kaya, T., "Mathematical Modeling of Loop Heat Pipes with Two-Phase Pressure Drop," AIAA Paper 99-3448, July 1999.